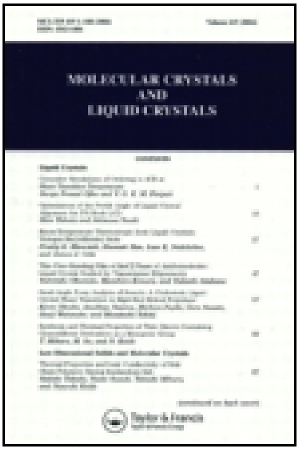

Molecular Crystals and Liquid Crystals Incorporating Nonlinear Optics
Publication details, including instructions for authors and subscription information:
http://www.tandfonline.com/loi/gmcl17

Electrohydrodynamic Instability in 8CB (4′-n-Octyl-4-Cyanobiphenyl) Liquid Crystal

D. K. Rout [a] & R. N. P. Choudhary [a]

[a] Department of Physics and Meteorology, Indian Institute of Technology, Kharagpur, 721302, India

Version of record first published: 19 Dec 2006.

To cite this article: D. K. Rout & R. N. P. Choudhary (1988): Electrohydrodynamic Instability in 8CB (4′-n-Octyl-4-Cyanobiphenyl) Liquid Crystal, Molecular Crystals and Liquid Crystals Incorporating Nonlinear Optics, 154:1, 241-258

To link to this article: http://dx.doi.org/10.1080/00268948808078734

Mol. Cryst. Liq. Cryst., 1988, Vol. 154, pp. 241–258
Photocopying permitted by license only

Printed in the United States of America

Electrohydrodynamic Instability in 8CB (4′-*n*-Octyl-4-Cyanobiphenyl) Liquid Crystal

D. K. ROUT and R. N. P. CHOUDHARY

Department of Physics and Meteorology, Indian Institute of Technology, Kharagpur-721302, India

(*Received June 22, 1987; in final form September 1, 1987*)

Electrohydrodynamic instability in homeotropic nematic samples of 8CB (4′-*n*-octyl-4-cyanobiphenyl) has been observed. Some similarities between this instability and thermally induced instability have been found in our investigations. The charge injection due to thermionic emission and diffusion current play an important and major role in the roll type cellular domains observed in electrohydrodynamic instability.

Keywords: 8CB, nematic, electrohydrodynamic instability, Felici–Benard instability, charge injection, diffusion process

I. INTRODUCTION

Extensive studies have already been made on the electrohydrodynamic (EHD) instability of many nematic liquid crystals having negative dielectric anisotropy for homogeneously aligned samples. The domain pattern was first observed in a sandwiched nematic film between two SnO_2 electrodes under a DC or AC field by Williams and co-worker.[1–3] Their conclusions in regard to the appearance of domains due to ferroelectricity were quite erroneous. Meyer later gave a theory of the piezoelectricity in nematic liquid crystals and explained it as a result of a static deformation of director caused by curvature electricity without flow motions.[4] Carr[5] had explained the occurrence of domains as a result of EHD instabilities in anisotropic fluids. Now, it is well known that the coupling effects between the space charge induced by director fluctuations, the convective flow of liquid crystals caused by the coulomb forces and the director motions are the major causes for the dissipative structures, which are known as Carr-Helfrich Instability (CHI).[5,6] The analogy between the EHD instability in nematic liquid crystals and in classical isotropic liquid has already been shown.[7,8] As we know, in isotropic liquid there exists the convective flow accompanied with the instability which has been considered as Felici Instability (FI).[9] CHI is essentially different from that of FI. While CHI occurs only in case of the nematic phase, FI occurs in both nematic and isotropic phases. It is also important to point out that, unlike CHI, FI does not occur when an AC field is applied. This indicates that FI does not exist without the charge injection from the electrode surface. The effects of the production of ions in a cell under a DC electric field were studied by Heilmeier *et al.*[10,11] Also, Rondelez showed that the charge injection at the boundaries is suppressed as soon as the oscillation frequency of the applied field exceeds a few cycles.[12] Therefore, there is a clear distinction between the mechanisms of instabilities arising due to the DC and AC excitation.

However, the EHD instability which occurred in a nematic sample having positive dielectric anisotropy is different from that of the negative dielectric anisotropy. For the first time, cellular domains were observed in the 5CB (pentyl-cyanobiphenyl) compound by Nakagawa *et al.*[13] They concluded that the instability could be explained as Felici–Benard instability (FBI). In order to verify these newly observed domain patterns and their mechanisms, we have studied the details of the EHD instabilities in 8CB, which is a higher homologue in the cyanobiphenyl group of compounds.

II. EXPERIMENTAL

Mesophase transitions of 8CB ($K \xrightleftharpoons{21.5°C} SmA \xrightleftharpoons{33.5°C} N \xrightleftharpoons{40.5°C} I$) were found to be the same as the reported values.[14] For electrical measurements, we used SnO_2-coated glass plates in which the sample was sandwiched. Mylar spacers were used to determine the thickness. Homeotropic alignment was obtained by pre-treating the glass plates with CTAB (Cetyl Trimethyl Ammonium Bromide). The temperature during the measurement was controlled with the help of an Indotherm temperature controller (model 401) and a hot stage designed by us (Figure 1).

The hot stage was mounted on a Censico polarising microscope stage for visual observation as well as microphotographic work. Heat

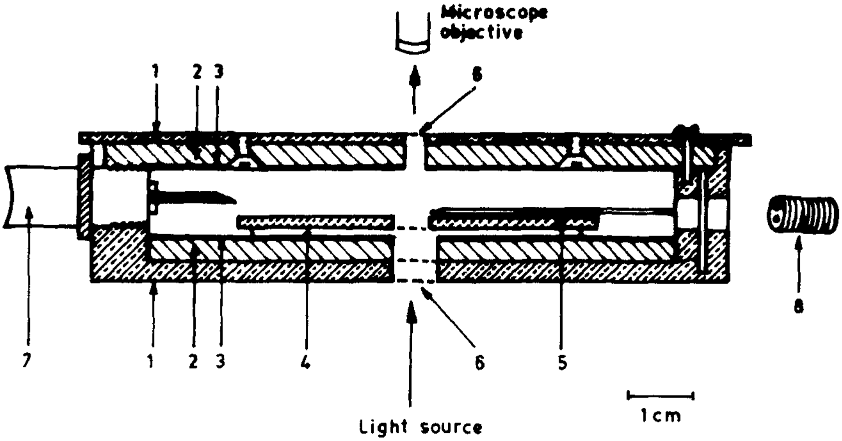

FIGURE 1 Hot stage for microscopic observation as well as electrical measurements. 1. Brass; 2. Asbestos; 3. Mica; 4. Heater; 5. Heating plate (aluminium); 6. Heat resisting glass; 7. BNC probes; 8. Inlet of power and thermocouple circuits.

resisting glasses were used in the hot stage to prevent a thermal gradient along the passage of light. The observation of the displacement of the nematic–isotropic interface with temperature showed the temperature gradient to be less than 0.5°C/min. The sample temperature was measured by a chromel–alumel thermocouple located near the lower glass plate of the sample cell.

DC voltage was applied to the sample cell with an Aplab power supply and the current flow was measured with the help of a DC nanometer. The diffusion process was studied by the current transient technique. The switching transients were recorded after a DC step voltage of 2 volts was switched on and off across the sample cell. The recording was performed with a digital memory-scope (Iwatsu DMS-6430) at a clock rate of 10 μs per WD and a data length of 1024 WD.

III. RESULTS AND DISCUSSION

a) Microscopic observation

Figure 2b shows the gradual appearance of domains with the increase of applied DC voltage. The sample thickness (50 μ) was determined by mylar spacers. The magnification in the present case was ×395 and the analyser and polariser were kept crossed. The homeotropic

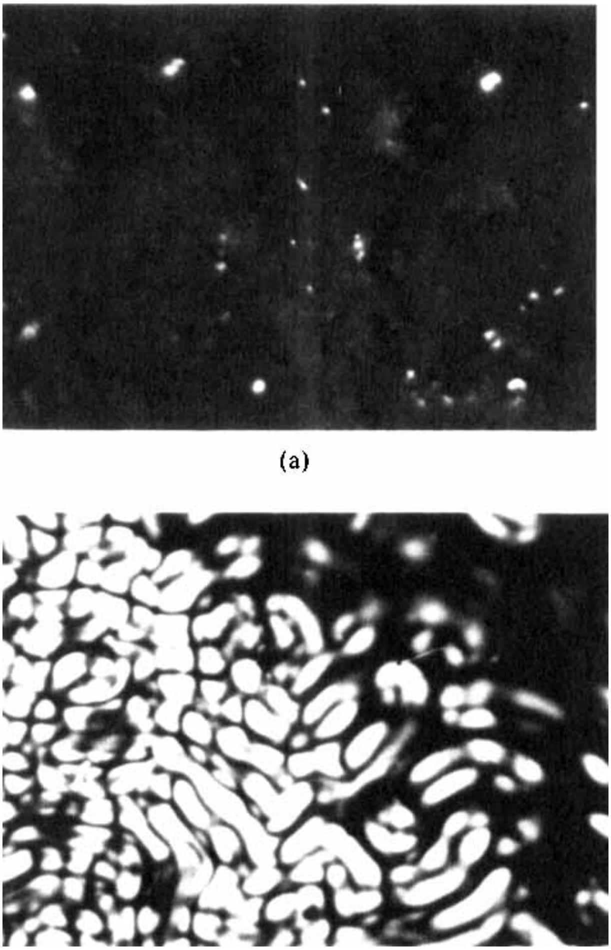

(a)

(b)

FIGURE 2 The onset of domains with the increasing applied voltage (a) V = 0 V, (b) V = 4 V, (c) V = 5 V, (d) V = 6 V, (e) V = 8 V, (f) V = 10 V, (g) V = 11 V.

alignment was quite good as evident from Figure 2a. The temperature maintained during the observation was 37°C. With the increase of the applied voltage, the cellular domains start to appear at a threshold voltage $V_{TH} \simeq 4$ volts (Figure 2b). The dark lines represent the homeotropic alignment at their centres. The domain boundaries also have homeotropic alignment as they are dark similar to the domain centres. With the further increase of the applied voltage, two neighbouring domains are fused into an elongated roll like structure (Figure

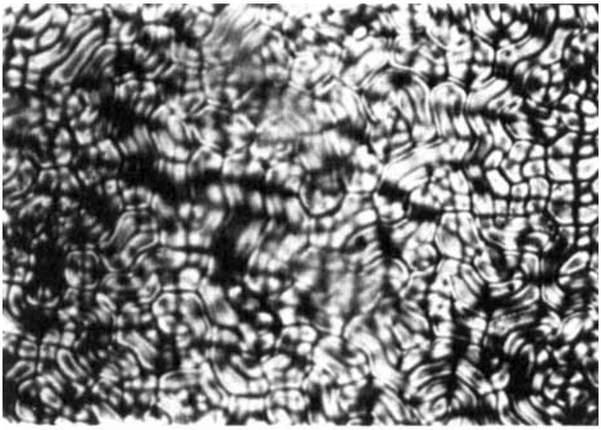

(c)

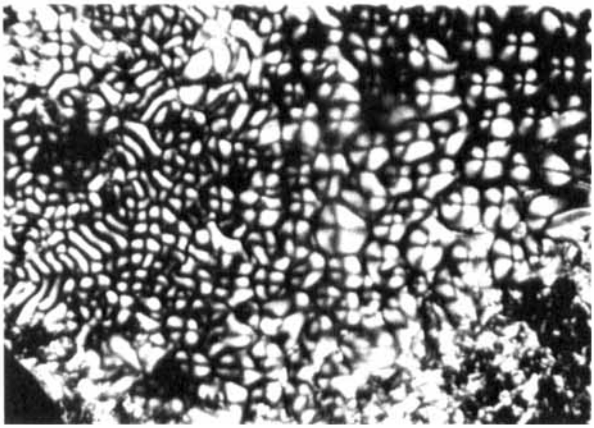

(d)

FIGURE 2 (*continued*)

2c). When the applied voltage was increased to 6 volts, partial fluctuation of the dissipative structure starts, as a result of which the size of the domains become more irregular (Figure 2d, e). The fluctuations of the dissipative structure become more prominent with the increase of the applied voltage. When the applied voltage exceeds 10 volts ($E = 2\,\mathrm{kV\,cm^{-1}}$), it is no longer possible to observe the usual cellular roll like domains (Figure 2c). Instead, only the cross-like isogyres appear (Figure 2f, g) except for some places, where the cellular pattern is still visible. This phenomenon is understood to be the result

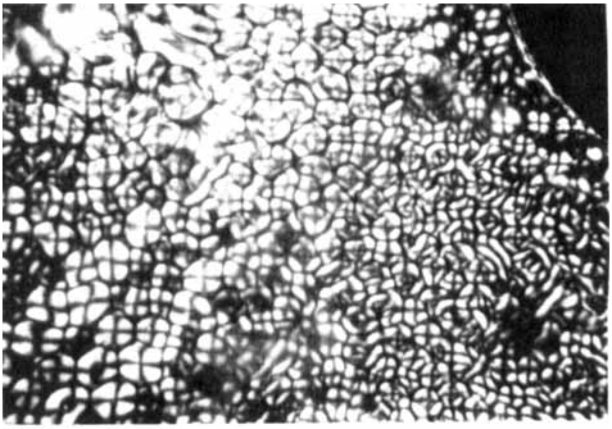

(e)

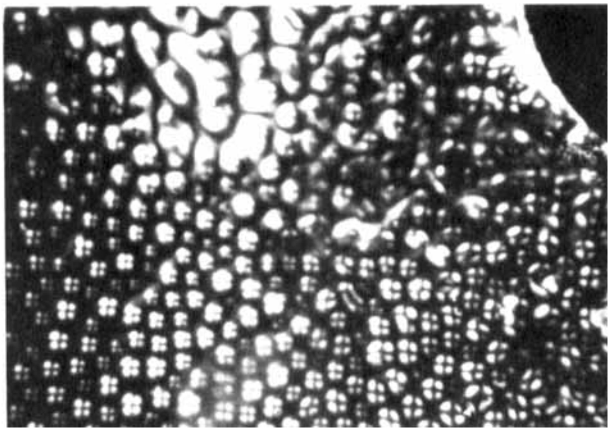

(f)

of sample degradation due to an electrochemical reaction under high electric field. These phenomena are analogical to the cellular convections in fluids first observed by Benard.[19] Here it is quite clear that at higher fields we are not able to get the dynamic scattering mode (DSM) type of turbulent behaviour but only fluctuations of the dissipative structure. We also found a periodic flow of odd dust particles between a domain centre and domain boundary. The dimension of the domain is found to be dependent on the cell thickness.

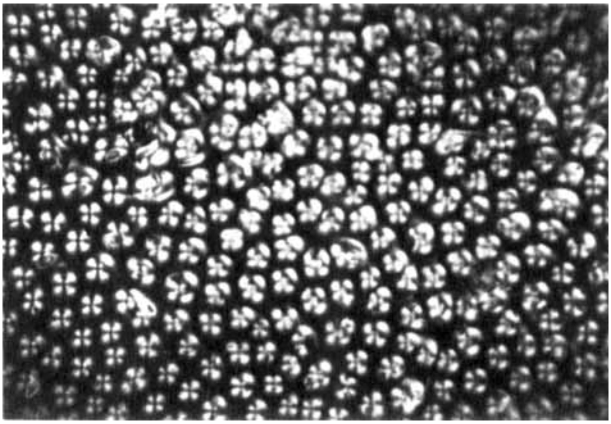

(g)

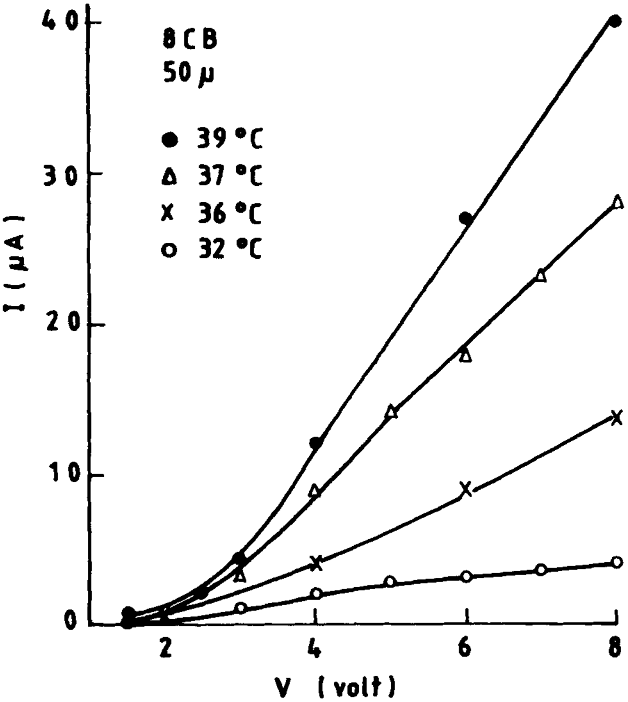

FIGURE 3 I-V characteristics at different temperatures for the 50 μ thick 8CB sample.

b) Electrical measurements

(i) Existence of the charge injection. Figure 3 and Figure 4 show the variation of current with voltage as a function of temperature for the sample thickness 50 μ and 75 μ respectively. The values of current increase after the SmA–N transition. In the SmA phase, the current does not change much with the increasing voltage in contrast to the nematic phase.

Figure 5 and Figure 6 show the variation of current in the SmA and N phases with temperature at different voltages. The current values increase rapidly at the time of the onset of domains. When instability occurs, the flow of current increases. We have not observed the thermally induced hysteresis phenomena as reported by Nakagawa *et al.*

As has been found experimentally[15,16] in a nematic cell under a DC field, the charge injection from the electrodes becomes significant

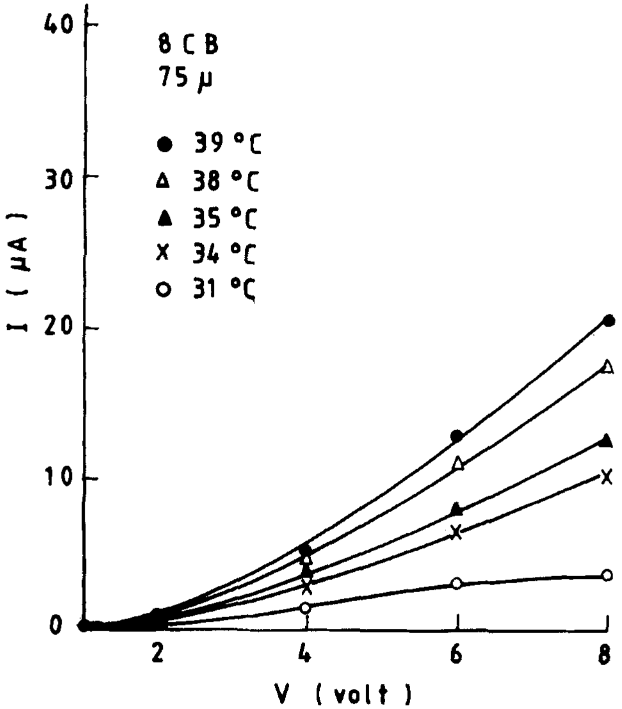

FIGURE 4 I–V characteristics at different temperatures for the 75 μ thick 8CB sample.

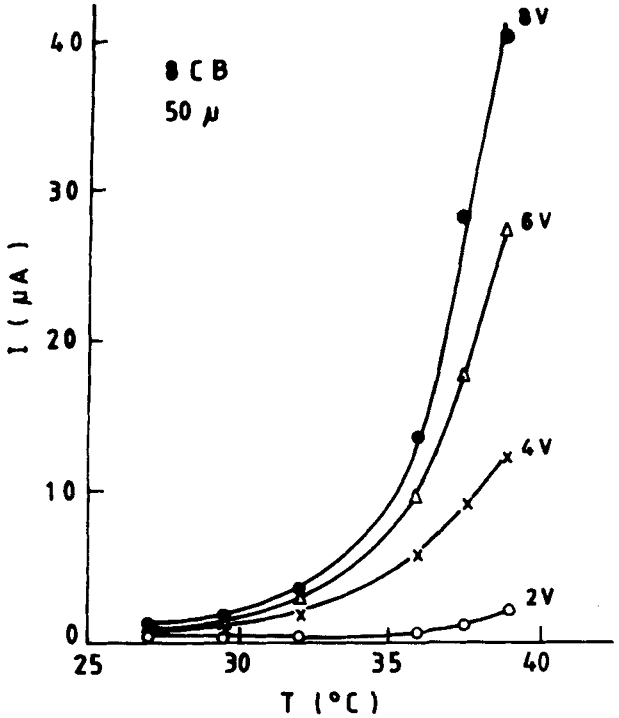

FIGURE 5 The dependence of current on temperature at various applied voltages for the 50 μ thick 8CB sample.

enough to explain instabilities such as FI.[17] We assume the above facts in our present experiment. Thus, we observe the increase of current due to carrier injection with the increase of temperature. We further take the assumption of Nakagawa *et al.* that the current density J through the sample follows Richardson's emission law

$$J = AT^2 \exp(-\phi/kT) \tag{1}$$

where T is the absolute temperature, k is Boltzmann's constant, A is a constant and ϕ is the thermionic work function. Both A and ϕ depend on the materials of the electrode, surface preparation and the applied electric fields. Following Eq. (1) we plotted log I/T^2 versus $10^3/T$ (Figures 7, 8) from the experimental data of Figures 5 and 6 for 50 μ and 75 μ thick samples of 8CB respectively. The discontinuity at the SmA–N phase transition is clearly observed. The slope of the

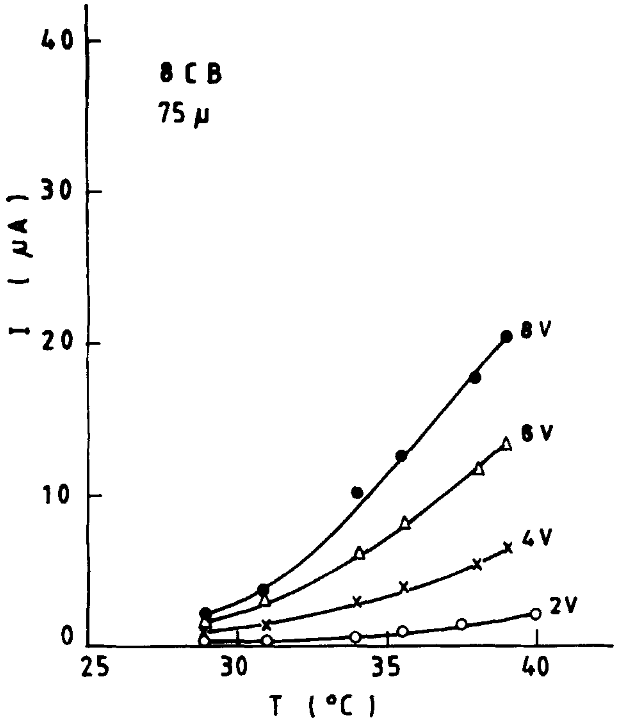

FIGURE 6 The dependence of current on temperature at various applied voltages for the 75 μ thick 8CB sample.

lines in the SmA phases decreases with decreasing temperature. At low temperatures in the SmA phase, the slopes become almost constant. The work function ϕ of the electrode (SnO_2) was calculated from the slopes of the log (I/T^2) vs $10^3/T$ (Figures 7, 8). From the voltage dependence of ϕ (Figure 9), we found that ϕ decreases with the increase of the applied field in contrast to the observation of Nakagawa *et al.* on 5CB.[13] In their case, the ϕ first increases up to 4 volts and then decreases. This lowering of the work function of the electrode material can arise from the existence of an electrical double layer near the electrode surface. Even before the occurance of cellular domain pattern (i.e. before $V_{TH} \simeq 4$ volts), isogyres start to appear and hence, the formation of the double layer before V_{TH} cannot be ruled out. The charge carriers are also of extrinsic nature which has not been explained earlier.

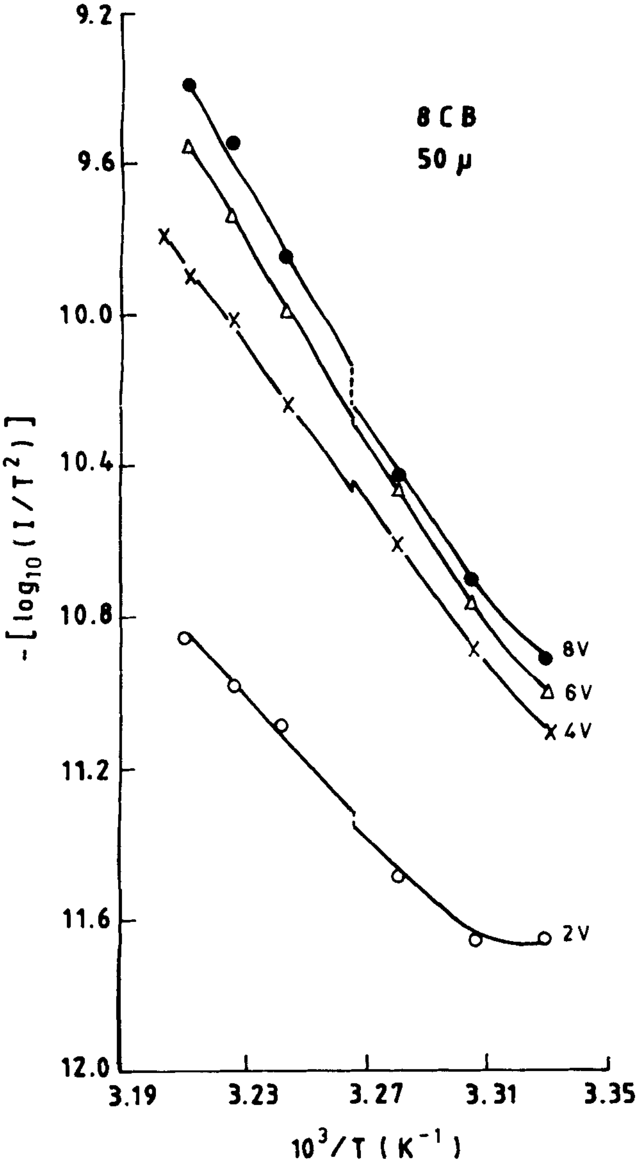

FIGURE 7 The plots of $-(\log_{10} I/T^2)$ vs. $10^3/T$ at various applied voltages for the 50 μ thick 8CB sample.

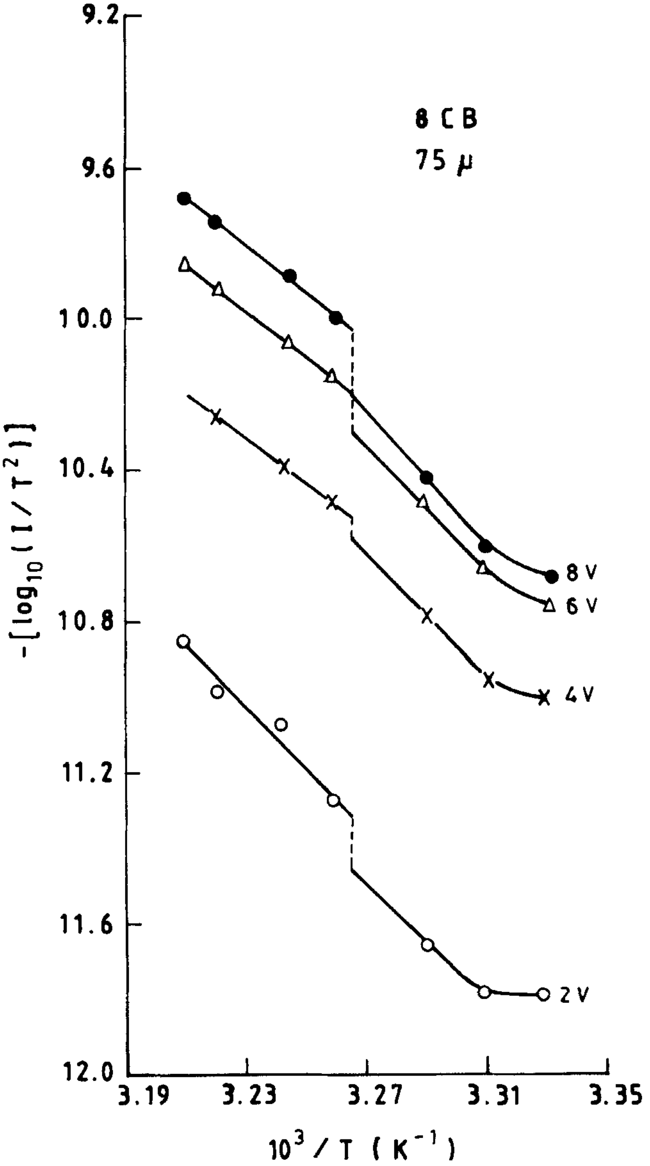

FIGURE 8 The plots of $-(\log_{10} I/T^2)$ vs. $10^3/T$ at various applied voltages for the 75 μ thick 8CB sample.

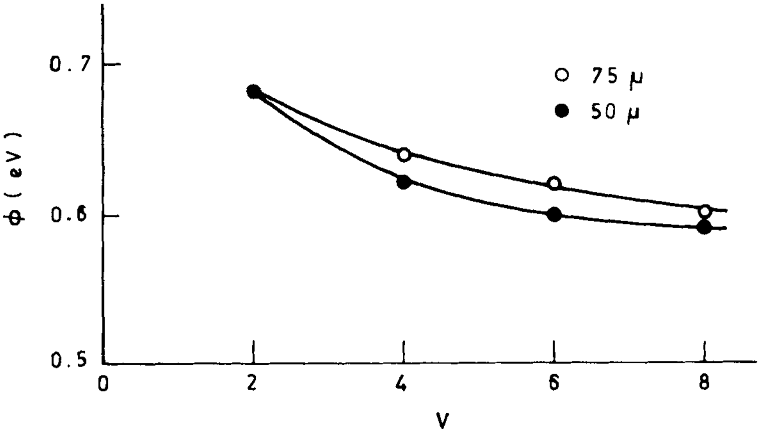

FIGURE 9 The voltage dependence of the thermionic emission work function.

(ii) Existence of the diffusion process

As mentioned by Nakagawa *et al.*, the dependence of current flow on the frequency of an applied AC field shows a slow relaxation ($\sim10^2$ sec.) process which is not due to dielectric relaxation ($\sim10^{-3}$ sec.). This long relaxation time may be explained as a result of the diffusion process. Chang *et al.*[18] also showed in their experiments that the decay time

$$T_D = L^2/D\pi^2 \tag{2}$$

where L = sample thickness, D = diffusion constant is inversely proportional to the diffusion constant. From the above relation the characteristic decay time, as a result of a diffusion process, was found to be on the order of 10^2 seconds. In cases where the dielectric relaxation process is solely responsible for the present phenomena, the current flow $I(t)$ decreases exponentially as

$$I(t) \; \alpha \; \exp(-t/\tau) \tag{3}$$

where t, the time after the applied voltage is removed and τ, the dielectric relaxation time. On the other hand, if the diffusion process is mainly responsible, for large t, $I(t)$ has the form of

$$\mathrm{I}(t) \; \alpha \; (\mathrm{D}/t)^{1/2} \tag{4}$$

This type of relation has also been shown by Ulhir[19] in his work on the temperature dependence of the saturation current for the anodic process in germanium with 10% KOH solutions. He has shown that $I = qp_o(D/\tau)^{1/2}$ where q = electronic charge and p_o = equilibrium hole concentration. He also mentioned the validity of the above relation for semiconducting materials of $\phi \sim 0.7$ ev. In our case, the ϕ value was found to be ~ 0.6 ev.

To examine which of the above processes is dominant in 8CB, we studied the transient phenomena of the current flow in it after the field was removed. For this purpose, we applied a step voltage of 2 V which is below the threshold value for hydrodynamic instability so that we could eliminate the hydrodynamic effects. The traces of the current transients were taken directly from the memory-scope screen and are produced here in Figure 10. The transients were taken at different temperatures throughout the nematic as well as smectic phases. These results clearly show that $I(t)$ does not follow Equation 3. From the $I(t)$ vs. $t^{-1/2}$ curves in (Figure 11 and Figure 12), we find that Equation 4 holds good for $t \gtrsim 1.5$ sec (50 μ sample). This result

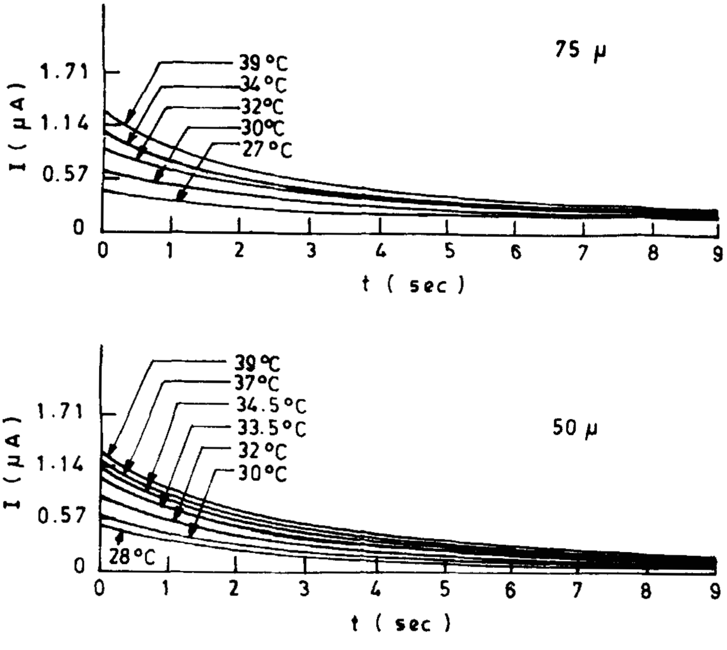

FIGURE 10 The transient currents for 8CB at different temperatures.

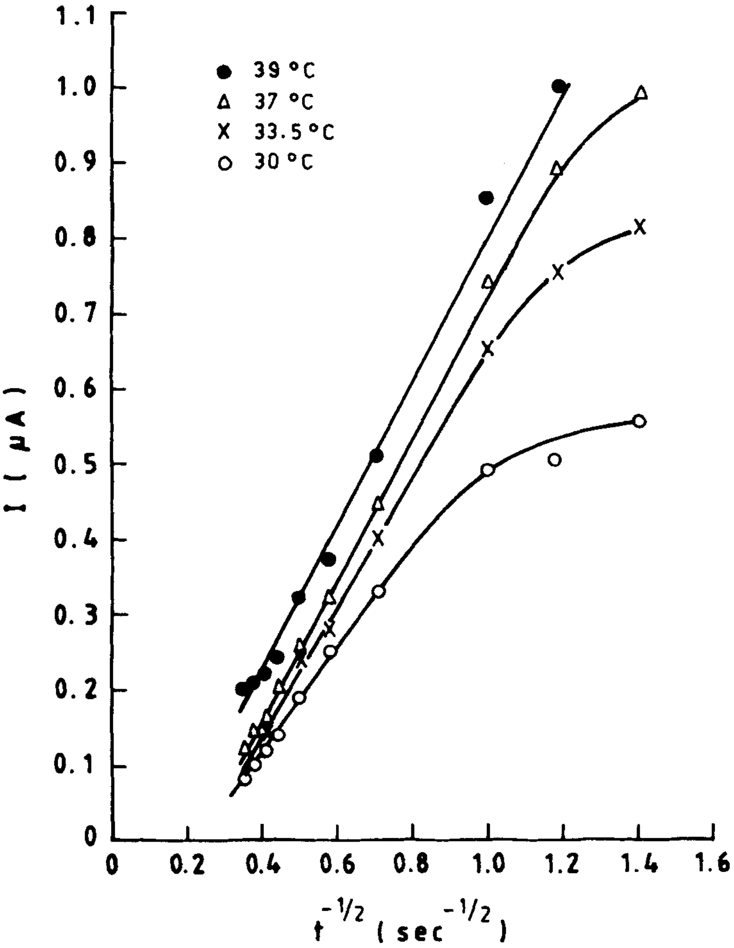

FIGURE 11 The plots of $I(t) - t^{-1/2}$ for the 50 μ 8CB sample.

just indicates the validity of our assumption regarding the existence of the diffusion process. Further we found that this time limit depends upon the sample thickness. For a 75 μ thick sample, Eq. (4) holds good for $t \gtrsim 2.7$ sec. However, the deviation from the linear relationship for a lower t is attributed partially to the dielectric relaxation process which should appear for a lower t. In our experiments, we have verified the assumptions of the existence of a charge injection due to the thermionic emission process at the boundaries and of the diffusion process. We obtained relatively high values of current in

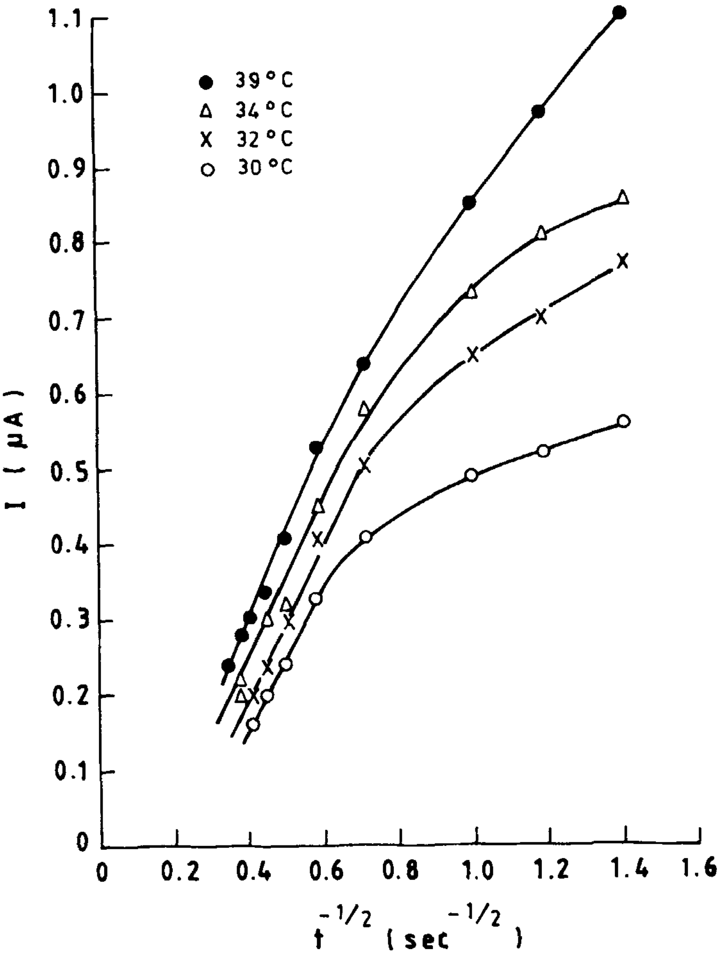

FIGURE 12 The plots of $I(t) - t^{-1/2}$ for the 75 μ 8CB sample.

comparison to those observed by Nakagawa *et al.* Our method of surface preparation of the electrode for the homeotropic alignment may be responsible for such high values.

There is a report on the existence of hysteresis phenomena in the I–V characteristics of 5CB but here is not observed by us. When the applied voltage approaches the V_{TH}, the ions start to accumulate at the boundaries as a result of convective flow and an internal field is set up. If the assumption of unipolar charge injection is correct, the total current will be the sum of the conduction and diffusion current.

We believe that the hysteresis in I–V characteristics should not be observed if the rate of application of voltage to the sample and the time of observation of current after the voltage switched on is kept uniform throughout the experiment.

We also observed that above V_{TH} (~8 volts) the current slowly decreases with time, which often causes difficulty in measurement. This type of behaviour is due to the fact that after switching on the applied voltage, the initial current decreases relatively faster because of the space charge formation for a short time. Then it decreases very slowly due to the diffusion of ions. As diffusion progresses the carriers are swept out of the dielectric and then the current decreases to a steady state. The time needed for a steady state current again depends upon the temperature and structural phase. In our present experiment, we measured the current 15 seconds after switching on the voltage across the sample. Similarly, we recorded the current transients one minute after switching on the voltage.

V. CONCLUSIONS

The assumptions regarding the occurrence of the present instability i.e. the existence of charge injection, diffusion process and fluid flow are found to be correct in our experiments. In addition to these we found that the charge carriers are extrinsic in nature. Above a certain field applied to the sample, an electrochemical reaction takes place resulting in a greying appearance in the sample. The existence of double layers between the electrodes and the liquid crystal has been shown clearly in our experiments. We have not observed any domain pattern in the isotropic liquid phase.

Acknowledgments

The authors wish to acknowledge their gratefulness to M/s BDH Ltd., England, for providing the sample. One of us (D. K. R.) is grateful to CSIR, New Delhi for a research fellowship. We also thank Prof. K. V. Rao for his kind help and encouragement during the work.

References

1. R. Williams, *J. Chem. Phys.*, **39**, 384 (1963).
2. R. Williams and G. Heilmeier, *J. Chem. Phys.*, **44**, 638 (1966).
3. R. Williams, *Advan. Chem. Ser.*, **63**, 61 (1967).

4. R. B. Meyer, *Phys. Rev. Lett.*, **22**, 918 (1969).
5. E. F. Carr, *Adv. Chem. Ser.*, **63**, 86 (1967).
6. W. Helfrich, *J. Chem. Phys.*, **51**, 4092 (1969).
7. S. Kai and K. Hirakawa, *J. Phys. Soc. Japan*, 301 (1976).
8. K. Hirakawa and S. Kai, *Mol. Cryst. Liq. Cryst.*, **40**, 261 (1977).
9. H. Koelmans and A. M. Boxtel, *Phys. Lett.*, **326**, 32 (1976).
10. G. H. Heilmeier, L. A. Zanoni and L. A. Barton, *Proc. IEEE*, **56**, 1162 (1968).
11. G. H. Heilmeir, L. A. Zanoni and L. A. Barton, *IEEE Trans.* ED-17, 22 (1970).
12. F. Rondelez, Thesis, Université de Paris, Orsay (1970).
13. M. Nakagawa and T. Akahane, *J. Phys. Soc. Japan*, **11**, 33773 (1983).
14. As per data given by M/s B.D.H. Co., England.
15. H. Gruler and G. Meier, *Mol. Cryst. Liq. Cryst.*, **12**, 289 (1971).
16. P. A. Penz, *Mol. Cryst. Liq. Cryst.*, **141**, 15 (1971).
17. N. Felici, *Rev. Gen. Elect.*, **78**, 717 (1969).
18. T. S. Chang, P. E. Greene and E. E. Loebner in "Liq. Cryst. and Ordered Fluids," Vol. 2, edited by J. F. Johnson and R. S. Porter, p. 115.
19. Uhlir, A., *Bell Systems Tech. J.*, **35**, 333 (1956) in "Semiconductors" edited by N. B. Hannay, ch. 17, (1959).
20. H. Benard, *Annales de Chimie et de Phys.*, **23**, 62 (1901).
21. S. Chandrasekhar, *Hydrodynamic and Magnetic Stability*, Oxford, 1961, ch. 2.